Published in final edited form as:
J Control Release. 2012 May 10; 159(3): 362–367. doi:10.1016/j.jconrel.2012.02.030.

Doxorubicin-conjugated chimeric polypeptide nanoparticles that respond to mild hyperthermia

Jonathan R. McDaniel[1], **Sarah R. MacEwan**[1], **Mark Dewhirst**[1,2], and **Ashutosh Chilkoti**[1,*]

[1]Department of Biomedical Engineering, Duke University, Durham, North Carolina, 27708-0281, USA.

[2]Department of Radiation Oncology, Duke University, Durham, North Carolina, 27708-0281, USA.

Abstract

This paper reports the design, physicochemical characterization and *in vitro* cytotoxicity of a thermally responsive chimeric polypeptide (CP), derived from an elastin-like polypeptide (ELP). The CP self-assembles into ~40 nm diameter nanoparticles upon conjugation of multiple copies of doxorubicin (Dox), and displays a nanoparticle-to-aggregate phase transition between 39–42 °C in media, a temperature range suitable for mild hyperthermia of solid tumors. The CP-Dox nanoparticle is stable upon dilution to low micromolar concentrations, and is cytotoxic at both 37 and 42 °C. A thermally responsive nanoparticle formulation of Dox may prove to be broadly useful in hyperthermia targeted chemotherapy of a variety of solid tumors.

Keywords

Elastin-like polypeptide; hyperthermia; targeting; nanoparticle; thermosensitive; cancer; tumors

1. Introduction

We have recently developed a class of recombinant chimeric polypeptides (CPs) for delivery of small molecule chemotherapeutics. CPs have two components: (1) the N-terminal segment is a hydrophilic elastin-like polypeptide (ELP), a class of macromolecular carriers inspired by tropoelastin, which consists of multiple repeats of Val-Pro-Gly-Xaa-Gly, where the guest residue “Xaa” is any amino acid except proline [1, 2]; and (2) the C-terminal segment contains a variable number of periodically spaced cysteine (Cys) residues arranged in a Cys-(Gly-Gly-Cys)$_n$ motif to which small molecule chemotherapeutics can be attached. We have shown that the attachment of multiple copies of doxorubicin (Dox) to Cys residues at the C-terminus of a recombinant CP results in the spontaneous self-assembly of CP-Dox conjugates into near monodisperse nanoparticles, such that Dox is sequestered in the nanoparticle core while the hydrophilic CP forms the hydrated nanoparticle corona [3]. In this scheme, Dox is attached to a CP through an acid-labile hydrazone linker to enable intracellular release of the drug within acidic compartments such as endosomes and

*Corresponding author: chilkoti@duke.edu, Phone: (919) 660-5373.

Associated Content

Supporting Information. Experimental procedures; oligomer sequences; transition temperatures.

lysosomes. Notably, we find that nanoparticles of the CP-Dox conjugate accumulate in tumors at higher levels than free drug, and show good efficacy in a *s.c.* murine model of a colon carcinoma [3]. In the next stage of evolution of these drug-loaded nanoparticles, we are interested in improving their accumulation in solid tumors by "active" targeting.

Affinity targeting is the most common approach for "active" targeting of nanoparticles, in which the nanoparticle exterior is decorated with tumor specific ligands such as antibodies and their fragments [4–7], or aptamers [8] that interact specifically with high affinity receptors over-expressed by a tumor [9]. Conventional receptor-targeted drug delivery has several limitations: (1) the spatial heterogeneity of receptor expression within a tumor [10–12], between patients with the same cancer [13], and across tumor types [14] limits application of an affinity targeted drug carrier to a narrow range of tumors that overexpress the target receptor; (2) expression of the target receptor in healthy tissues at baseline levels leads to significant off-site targeting and hence, systemic toxicity.

These limitations of affinity targeting have led us to investigate an alternative, receptor independent physical-targeting approach that takes advantage of focused mild hyperthermia of solid tumors by "thermally" targeting CP-Dox nanoparticles to tumors. This goal is motivated by previous studies that showed that triggering the phase transition of an ELP can increase its accumulation in solid tumors that are externally heated by mild hyperthermia [15–17]. CPs can be used to build a thermally-responsive nanodelivery system because they –similar to the ELPs that they are derived from– undergo a lower critical solution temperature (LCST) phase transition, defined by an inverse transition temperature (T_t), or LCST, below which a CP is soluble and above which the CP desolvates and forms micron-sized aggregates.

CP-Dox nanoparticles also undergo a phase transition in response to an increase in temperature, causing the CP-Dox nanoparticles to collapse into micron-sized aggregates. This transition is also defined by a T_t, which is the solution temperature for the onset of aggregation of CP-Dox nanoparticles. The T_t of the CP-Dox nanoparticles in our previous study was above the upper limit of 42 °C that is necessary for targeting by externally-focused mild hyperthermia [3], so that those nanoparticles were not useful for thermal targeting of solid tumors. However, the T_t of CP-Dox nanoparticles, like the CPs from which they are derived, can be tuned by controlling the CP composition and chain length, which provides a rational approach for the design of a CP that responds to mild hyperthermia. In an effort to improve the therapeutic efficacy of CP-Dox nanoparticles, we report herein the design, physico-chemical characterization, and *in vitro* cytotoxicity of a thermally responsive CP-Dox nanoparticle that undergoes a transition from a nanoparticle to a microscopic aggregate in response to mild hyperthermia under physiological conditions.

2. Material and Methods

2.1 Materials

Restriction enzymes, T4 DNA ligase and calf intestinal phosphatase (CIP) were purchased from New England Biolabs (Ipswich, MA). The pET-24a+ cloning vector was obtained from Novagen Inc. (Madison, WI), and all custom oligonucleotides were synthesized by Integrated DNA Technologies Inc. (Coralville, IA). The DNA miniprep, gel purification, and PCR purification kits were purchased from Qiagen Inc. (Germantown, MD). EB5α™ and BL21™ *E. coli* cells were purchased from Edge BioSystems (Gaithersburg, MD). All *E. coli* cultures were grown in TBDry™ media purchased from MO BIO Laboratories, Inc (Carlsbad, CA). Doxorubicin-HCl was purchased from Tecoland (Edison, NJ). BMPH and TCEP were obtained from Thermo Scientific (Rockford, IL). Kanamycin was purchased from CalBioChem (San Diego, CA).

2.2 Synthesis of chimeric polypeptides

CPs were synthesized from purchased oligomers using plasmid reconstruction recursive directional ligation (complete details can be found in the supporting information) [18]. The nomenclature used herein indicates the different CP sequences (1–4, determined by the guest residue composition). CPs conjugated to Dox (CP-Dox) imply nanoparticle formulations whereas unconjugated CPs are unimers. The T_t was tuned by varying the guest residue ratio of alanines to valines. The CP sequences that were synthesized in this study are shown in Table I.

2.3 Expression and purification of CPs

CPs indicated by an asterisk in Table I were expressed from a modified pET-24a+ expression vector [18], using a previously published hyperexpression protocol, which relies on the leakiness of the T7 promoter [19].

2.4 SDS-PAGE

SDS-PAGE of purified CPs was performed on Bio-Rad Ready Gels™ with a 4–20% Tris gradient. The gels were visualized by copper staining (0.5 M $CuCl_2$).

2.5 Conjugation of Dox to CP

The conjugation of Dox to the CPs was performed as described elsewhere [3]. The degree of Dox conjugation to the CP was measured for each sample by resuspending 10–20 mg of lyophilized CP-Dox in 1 mL of PBS, and then dividing the concentration of Dox, determined via absorbance spectroscopy, by the concentration of CP. The CP concentration was determined gravimetrically on the lyophilized sample by adjusting for the added mass from the attached Dox-linker.

2.6 Temperature programmed turbidimetry

The transition temperature (T_t) of each sample was calculated by recording the optical density at 650 nm as a function of temperature (1 °C/min ramp) on a temperature controlled UV-Vis spectrophotometer (Cary 300 Bio; Varian Instruments, Palo Alto, CA). The T_t was defined as the inflection point of the turbidity profile. All samples were analyzed in PBS or complete cell media (RPMI-1640 supplemented with 10% FBS, 4.5 g L^{-1} D-glucose, 10 mM HEPES, and 1 mM sodium pyruvate) across a wide range of CP concentrations (2 μM to 100 μM).

2.7 Light scattering

Dynamic light scattering (DLS) was performed to determine the hydrodynamic radius (R_h) of the CPs and CP-Dox nanoparticles at 25 μM CP concentration and 25 °C using a Dynapro plate reader (Wyatt Technology; Santa Barbara, CA), following filtration through 0.22 μm Millex-GV filters (Millipore; Billerica, MA). The data was analyzed with a regularization fit of the percent mass for Raleigh spheres. The ALV/CGS-3 goniometer system (Germany) was used to perform both dynamic and static light scattering. Samples for the ALV/CGS-3 goniometer system were prepared in PBS with 5 mM TCEP and filtered into 10 mm disposable borosilicate glass tubes (Fischer) that had been previously cleaned with filtered ethanol (0.2 μM cellulose acetate filter). Measurements were obtained at 25 °C for angles 30° – 150° at 5° intervals, with each measurement consisting of 3 runs sampled for 10 – 30 seconds each. The ALV Static and Dynamic Fit and Plot algorithm was used to fit partial Zimm plots for each concentration, providing the absolute molecular weight and the R_g. The R_g and R_h measured on the ALV/CGS-3 system were used to calculate the shape factor of CP-Dox nanoparticles.

2.8 Cytotoxicity

C26 murine colon carcinoma cells were maintained in complete media consisting of RPMI-1640 supplemented with 10% FBS, 4.5 g L^{-1} D-glucose, 10 mM HEPES, and 1 mM sodium pyruvate. Cells were maintained at 37 °C and 5% CO_2 and passaged every 3 days. *In vitro* cytotoxicity was determined through the use of a colorimetric assay. 5×10^3 C26 cells were seeded per 100 μL media on BD Falcon™ 96-well cell culture plates (BD; Franklin Lakes, NJ) and allowed to adhere for 24 h. The cell media was then removed and replaced with 120 μL complete media containing Dox, CP nanoparticles, or unconjugated CP. The plates were treated at 37 or 42 °C for 1 h, after which they were incubated at 37 °C for 24 to 72 h. The plates were then removed and 20 μL of CellTiter 96 AQueous™ (Promega; Madison, WI) 3-(4,5,-dimethyl2-yl)-5-(3-carboxymethoxyphenyl)-2-(4-sulfophenyl)-2H-tetrazolium (MTS) reagent was added to each well. Following incubation for 30 min, the absorbance of the solution was measured at 490 nm with a Victor^3 microplate reader (Perkin Elmer; Waltham, MA). To calculate the IC_{50}, the data was fit to the equation: Viability = $1 / (1 + (C_{Dox}/IC_{50})^p)$, where C_{Dox} is the effective Dox concentration in the well, the IC_{50} measures the necessary dose to kill 50% of the cell population, and p represents the slope of the sigmoidal curve.

2.9 Fluorescence microscopy

For visualization of Dox delivery with CP nanoparticles, 4×10^3 C26 cells were seeded on Lab-Tek® II CC2™ chamber slides (Electron Microscopy Sciences, Hatfield, PA) and allowed to adhere for 24 hours. Cell media was replaced with complete media containing CP nanoparticles and incubated for 1 hr at 37 °C or 42°C. Following treatment the media was removed and cells were incubated for 10 min with 2 μM Hoechst 33342 to stain cell nuclei. The cells were then washed twice in PBS at room temperature. Cells were fixed for 20 min in 4% paraformaldehyde and the chamber wells were removed from the underlying slide on which the cells were adhered. The slide was mounted with Fluoromount-G (Electron Microscopy Sciences, Hatfield, PA) prior to visualization on a Nikon TE-2000U widefield fluorescence microscope with a 60x oil-immersion objective. Hoechst 33342 dye was detected with a standard UV-2E/C filter set and Dox was detected with a 450–490 nm excitation filter, 505 nm long pass dichromatic mirror, and 590–650 nm emission filter set.

3. Results

We designed a family of CPs to precisely tune the phase transition behavior of CP-Dox nanoparticles, with the goal of identifying at least one CP that would provide a nanoparticle with a T_t within the required 39–42 °C upon Dox conjugation. This spans the temperature window from physiological conditions to mild hyperthermia. We chose the specific CP sequences for synthesis based on a large body of experimental evidence that we have collected in the past decade on the effect of two orthogonal variables – the guest residue and the molecular weight – on the T_t of ELPs [16, 20–22]. These studies suggest that different combinations of Val, Ala, and Gly residues at the 4th, guest residue position would yield CPs with a T_t of ~40 °C in a relevant physiological fluid such as plasma [16, 17].

Using this information as a guide, we synthesized 22 genes that encode four sets of CPs with varying guest ratios of valine (V) and alanine (A) and a range of MWs. Genes encoding low molecular weight constructs (MW < 15 kDa) were not expressed because low MW CPs tend to express with low yield and have very high T_t's. Of the remainder, 11 CPs were expressed in *E. coli* and were purified to homogeneity to determine how the T_t of these CPs varied as a function of their composition and molecular weight. We measured the T_t's of the 11 CPs in PBS to determine which CPs were likely to exhibit Tt's within the range of clinical

hyperthermia following assembly into nanoparticles. Based on their measured Tt's (SI Figure 2), we next conjugated one CP from each set of unique compositions to Dox.

Multiple copies of Dox were attached to the cysteine rich C-terminus of each CP to drive nanoparticle assembly, as previously described [3], using a pH-sensitive linker with an internal hydrazone bond that enables intracellular release of the drug from the CP under the conditions of low pH (<5.5) found in the endosomes and lysosomes [23]. Upon conjugation of multiple copies of Dox, all of the CP-Dox conjugates self-assemble into near-monodisperse spherical nanoparticles that are approximately 20 nm in radius (Table II). The degree of Dox conjugation per CP is also reported in Table II. Typically, the number of drug molecules conjugated per CP range from 5 to 6.5, which corresponds to 4–5 wt% loading of drug. We did not attempt to optimize the drug loading of these conjugates any further by tuning the number of reactive cysteine residues, as a single injection of a CP-Dox formulation with ~5 wt% loading of Dox proved to be remarkably effective in a previous study in abolishing a syngeneic colon carcinoma in a *s.c.* model in balb/c mice [3].

Next, we measured the T_t of the CP-Dox nanoparticles as a function of the CP concentration in PBS (Figure 1B) and in 90% FBS. The T_t of the CP-Dox nanoparticles is primarily a function of the CP composition rather than their concentration in the range of 1–100 μM, which is in sharp contrast to CP unimers (no Dox attached) whose transition temperatures vary significantly with their composition and concentration (Figure 1A). In PBS, the T_t of the CP-Dox nanoparticles ranged from 39.7 °C for CP4-Dox to 46.8 °C for CP1-Dox. We also examined the thermal response of the CP-Dox nanoparticles in 90% FBS (a close approximation to physiological conditions), with the expectation that the presence of serum proteins would lower the transition temperature. We found that the T_t of all four CP-Dox nanoparticles decreased by ~3.5 °C, consistent with previous results.

We chose CP4-Dox for the remainder of the *in vitro* studies performed herein, as its T_t was in the range of 39–42 °C in PBS (39.7 °C at 50 μM) and cell culture medium (40.4 °C at 50 μM). However, we recognize that its T_t of 36.5 °C in 90% FBS is too low for thermal targeting after systemic administration *in vivo*. As the other three CP-Dox nanoparticles exhibited phase transitions between 39.4 and 42.1 °C in 90% FBS, which approximates the environment in systemic circulation, we have in hand three potential CP-Dox nanoparticles that have the thermal profile to make them suitable for *in vivo* studies. Because of the extraordinary stringent design requirement imposed by the narrow 5 °C temperature range necessary for tumor targeting by mild hyperthermia, these results also highlight the importance of designing a library of CPs with a systematic difference in composition, and hence T_t, so as to ultimately provide one or more thermally responsive CPs that have the appropriate thermal profile for *in vivo* tumor targeting by externally applied, mild hyperthermia of solid tumors.

We next characterized the CP4-Dox conjugate (160 pentapeptides) in detail because its thermal properties are in the temperature range of mild hyperthermia. This conjugate forms nanoparticles with a radius of 23.6 ± 2.4 nm (Figure 2A). This size is optimal to exploit the EPR effect, which facilitates passive accumulation of macromolecular carriers in a tumor by extravasation through the nanoscale pores in the leaky tumor vasculature. While these pores can range in size up to 100's of nanometers [24, 25], mild hyperthermia dramatically increases the pore cutoff size –up to four-fold– in some tumors, so that hyperthermia can further amplify passive targeting [26]. The sub-100 nm size of these nanoparticles also suggests they will benefit from prolonged circulation, accumulate in solid tumors by virtue of their extravasation through the tumor vasculature, and then be degraded over time [27]. This is in contrast to other thermally responsive synthetic polymers, such as poly(N-

isopropylacrylamide) (polyNIPAAm), which can only be used at low molecular weights due to their lack of degradation *in vivo* [28, 29].

We next examined the thermal phase behavior of the CP4-Dox nanoparticles as a function of the CP concentration in more detail. The self-assembly of nanoparticles upon Dox conjugation to CPs has two important effects on its thermal behavior. First, the T_t of the nanoparticle is reduced with respect to the corresponding CP unimer at the same CP concentration (Figure 2B). This change in T_t is consistent with the conjugation of a hydrophobic entity to a CP, similar to the introduction of hydrophobic amino acids in the CP guest residue position. The second significant effect is that the concentration dependence of the CP-Dox nanoparticle T_t is drastically reduced as compared to CP unimers (Figure 2C). While the nanoparticle T_t (red) remains within the hyperthermia window (black lines) over a wide range in concentration, unimers (green, blue) only do so within a narrow concentration window. The green line represents the most commonly used ELP (a unimer) for thermal targeting in the literature [15–17, 30–32]. Clearly, this ELP would only exhibit thermal responsiveness to mild hyperthermia within a relatively small concentration range if it were injected *in vivo* as a unimer.

Chilkoti and Meyer defined the CP unimer T_t in terms of a critical T_t (T_{tc}; °C), the critical concentration (C_c; μM), the length of the sequence (L; pentapeptides), the concentration of the CP (C; μM), and k (°C), a proportionality constant (Equation 1) [22].

$$T_t = T_{t,c} + k/L \ \ln(C_c/C) \quad (1)$$

The T_t is highly sensitive to concentration changes at low concentrations and relatively insensitive to changes at higher concentrations because of the logarithmic dependence of the unimer T_t upon concentration (Figure 2D). In contrast, self-assembly of CPs into nanoparticles upon conjugation with Dox largely abolishes the dependence of the T_t on the CP concentration. We believe that this occurs because nanoparticle formation simply shifts the effective CP concentration from the low concentration regime into the high concentration regime over all concentrations, with the consequence that the concentration dependence of the CP is driven not by the overall nanoparticle concentration, but by the high local and invariant concentration of the CP in the CP-Dox nanoparticles. For instance, a simple calculation suggests that 20 CP chains packed within a 20 nm radius nanoparticle results in an effective local concentration of 1 mM. This effect is important because CPs are generally used at concentrations of 10–50 μM *in vivo*, placing them in the low concentration regime that makes their T_t very sensitive to concentration. In contrast, the T_t of CP-Dox nanoparticles, at the same 10–50 μM overall CP concentration, is largely insensitive to the CP-Dox concentration. This effectively means that the T_t of a CP-Dox nanoparticle is insensitive to its solution concentration (on a CP basis) as long as it remains above the critical aggregation concentration (CAC) of the nanoparticle.

We also studied how varying the stoichiometry of Dox influences the self-assembly of CP-Dox nanoparticles and their thermal behavior in aqueous solution. For instance, increasing the average number of Dox molecules conjugated to CP4 from 2.4 to 5.4 does not cause a statistically significant shift in the nanoparticle T_t, as the CP conjugated with 2.4 Dox per chain had a T_t of 40.3 °C ± 0.13 and the CP conjugated with 5.4 Dox per chain CP had a T_t of 40.0 °C ± 0.24 (two-tailed t-test, $p > 0.05$). This remains true as long as the conjugation ratio is sufficient to induce nanoparticle formation, as we observe that as few as 2.4 Dox/CP is sufficient to drive nanoparticle assembly. While the range of drug loading examined here only ranges from ~2–6 wt%, this insensitivity of the T_t on the precise degree of conjugation –as long as it is above the threshold required for self-assembly– is important as it makes the system robust enough to be used for thermal targeting for different levels of drug loading.

To calculate the critical aggregation concentration (CAC) of these nanoparticles, static light scattering (SLS) was performed on a dilution series of CP4, with and without attached Dox. Detailed SLS data are reported in the Supplementary Information (SI). The CAC describes the concentration at which aggregation occurs, below which only soluble polymer chains –unimers– are present. The number of CPs/NP ranged from 8.0 at 50 μM to 5.3 at 0.5 μM, the sensitivity limit of the instrument. The ratio of the R_g to the R_h –the shape factor– was averaged over 6 concentrations between 50 and 3 μM to yield the value 0.77 ± 0.1, closely approximating the theoretical value for a hard sphere (0.775). These data suggest that the CP-Dox nanoparticles are most likely star-like micelles [33], which is consistent with their short hydrophobic tail and much longer hydrophilic segment. While these data do not provide the precise CAC, they clearly indicate that the CAC is in the sub-micromolar concentration regime. The CP4 unimer exhibits an average aggregation number of 0.99 CPs/NP indicating that in the absence of Dox conjugation, the CP is, as expected, a unimer.

Next, we investigated the cytotoxicity of the CP-Dox nanoparticles at 37 and 42 °C. Fluorescence images of cells after 1 h incubation with CP4-Dox nanoparticles (30 μM Dox equivalent) at 37 or 42 °C (Figure 3A–B) illustrate that the second requirement of cellular uptake and drug release is also met. The conjugated Dox rapidly colocalized with the Hoechst nuclear stain with or without applied heat, indicating that the Dox was able to reach its site of action, presumably because the Dox was released from the CP due to the low pH of the endosome [23]. We next examined the thermal reversibility of the CP-Dox nanoparticles in physiological media. Figure 3C shows that the phase transition remains fully reversible and exhibits the desired T_t in complete cell media. Finally, the *in vitro* cytotoxicity of the CP-Dox nanoparticles was investigated by a cell viability assay. Figure 3D shows that over a concentration range greater than the CAC, the conjugated drug remains cytotoxic following cellular exposure to the nanoparticles over 1 hour at 42 °C. Upon extravasation from the tumor vasculature to the extravascular space of the tumor tissue, the CP concentration is expected to drop below the CAC, thereby inducing disassociation of the nanoparticles into unimers. Figure 3E–F shows that at low carrier concentrations, the drug conjugate has a similar IC_{50} value as the free drug, indicating that neither the biopolymer itself nor the conjugation chemistry adversely affects drug toxicity. This relationship was maintained after a 1 h exposure at 37 °C (IC_{50}: CP-Dox: 1.9 ± 0.5 μM; Dox: 0.3 ± 0.1 μM) or 42 °C (IC_{50}: CP-Dox: 1.5 ± 0.4 μM, Dox: 0.2 ± 0.1 μM). CP in the absence of conjugated Dox caused no toxicity over the equivalent CP range at either temperature (data not shown). These *in vitro* tests suggest that CP-Dox nanoparticles are thermally responsive delivery vehicles that can be taken up by cells at 37 and 42 °C, and release Dox into the nucleus, all of which are essential for future studies of the *in vivo* efficacy of this thermally targeted nanoparticle delivery system.

4. Discussion

We have previously shown that intravenously injected, thermally responsive ELPs allow thermal targeting of solid tumors by the application of mild hyperthermia to a solid tumor. This was achieved by tuning the ELP transition temperature between 39 °C (slightly above physiological temperature) and 42 °C (the temperature achieved with mild clinical hyperthermia) [34]. Because the physiological temperature is below the T_t, the ELP circulates systemically as a soluble unimer; upon reaching a heated tumor in which the temperature is above the T_t, the ELP undergoes its inverse phase transition and forms micron-sized aggregates that adhere to the tumor vasculature [16]. The localized aggregation of ELP in a tumor has been shown to increase uptake through two separate mechanisms. First, upon cessation of hyperthermia, the resolubilization of the ELP aggregates creates a steep transvascular concentration gradient that drives ELP extravasation into the tumor by diffusion. This effect was amplified by thermally cycling tumors in a two step process: (1)

inducing the accumulation of ELP aggregates by the application of mild hyperthermia to the implanted tumors; and (2) redissolving the ELP aggregates by turning off hyperthermia, which leads to an increase in drug accumulation within the tumor compared to passive diffusion under normothermic conditions or to a single cycle of hyperthermia [15]. Second, by complementary *in vitro* cell culture studies, we have previously shown that the combination of hyperthermia and thermally triggered aggregation of ELP unimers increases cellular uptake by 2-fold *in vitro*, mediated through the interactions of the hydrophobic microscopic ELP aggregates with the cell membrane [32].

While these results were encouraging, two limitations needed to be solved to move this system into relevant preclinical animal models. First, the *in vivo* demonstration of thermal targeting with ELPs was performed with polypeptides that lacked a relevant therapeutic cargo (typically fluorophore or radionuclides were used in these studies) and these markers were attached at low conjugation ratios (< 1 wt%) to a single reactive site on the ELP [15, 16, 30–32]. We solved this problem by converting the ELP into a chimeric polypeptide by appending a drug conjugation peptide segment that provides a tunable number of reactive sites (typically 8 per CP though this number can be increased at will) so as to increase the number of drug molecules conjugated per polypeptide chain.

The second problem –that of the steep dependence of the ELP transition temperature– was more critical, as it only provides a narrow temporal window in which focused mild hyperthermia of tumors could be applied, especially if repeated cycles of hyperthermia were required to increase the accumulation of the ELP within a tumor. This is because the temperature required to trigger aggregation of the ELP steeply increases as the ELP concentration within the blood is reduced through renal clearance, degradation, and normal tissue or tumor uptake. Once the transition temperature increases above the tumor temperature (42 °C) because of dilution effects, the ELP loses its thermal targeting capability. The self-assembly of a CP into nanoparticles upon the attachment of Dox provides a solution to this problem, as these drug-loaded nanoparticles display almost no dependence on concentration in their thermal phase behavior and enable a useful amount of drug (~5 wt%) to be loaded into the nanoparticle via chemical conjugation, a strategy that we have previously shown provides a nanoparticle formulation of Dox that is highly potent *in vivo* [3]. However, in that study, the CP-Dox nanoparticle was not designed for thermal targeting and consequently had a T_t that was far too high to be useful for tumor targeting by mild hyperthermia. To address this limitation, we have shown herein that the CP can be redesigned to display a thermally triggered phase transition from nanoparticles to microscopic aggregates in a physiological milieu in response to mild hyperthermia, without compromising drug loading, stability, or cytotoxicity. These attributes will finally allow us to exploit thermal targeting for the *in vivo* delivery of chemotherapeutics to solid tumors in relevant preclinical animal models. These studies are currently in progress.

Supplementary Material

Refer to Web version on PubMed Central for supplementary material.

Acknowledgments

This work was partially supported by a grant from the National Institutes of Health (R01 EB000188) to A.C. and by the Triangle MRSEC though a DMR MRSEC grant to Duke University. J.R.M. acknowledges the financial support of a NIH Biotechnology Predoctoral Fellowship (T32 GM 8555). S.M acknowledges the support of the NSF MRSEC through a graduate fellowship. We thank C. Radford for assistance with synthesis of CPs used in this study.

References

1. Gray WR, Sandberg LB, Foster JA. Molecular model for elastin structure and function. Nature. 1973; 246(5434):461–466. [PubMed: 4762195]
2. Tatham AS, Shewry PR. Elastomeric proteins: Biological roles, structures and mechanisms. Trends Biochem Sci. 2000; 25(11):567–571. [PubMed: 11084370]
3. MacKay JA, Chen MN, McDaniel JR, Liu WG, Simnick AJ, Chilkoti A. Self-assembling chimeric polypeptide-doxorubicin conjugate nanoparticles that abolish tumours after a single injection. Nature Mat. 2009; 8(12):993–999.
4. Jaracz S, Chen J, Kuznetsova LV, Ojima L. Recent advances in tumor-targeting anticancer drug conjugates. Bioorgan Med Chem. 2005; 13(17):5043–5054.
5. Nellis DF, Giardina SL, Janini GM, Shenoy SR, Marks JD, Tsai R, Drummond DC, Hong K, Park JW, Ouellette TF, Perkins SC, Kirpotin DB. Preclinical manufacture of anti-her2 liposome-inserting, scfv-peg-lipid conjugate. 2. Conjugate micelle identity, purity, stability, and potency analysis. Biotechnol Progr. 2005; 21(1):221–232.
6. Torchilin VP, Lukyanov AN, Gao ZG, Papahadjopoulos-Sternberg B. Immunomicelles: Targeted pharmaceutical carriers for poorly soluble drugs. Proc. Natl. Acad. Sci. U. S. A. 2003; 100(10): 6039–6044. [PubMed: 12716967]
7. Zhou Y, Daryl C, Zou H, Hayes ME, Adams GP, Kirpotin DB, Marks JD. Impact of single-chain fv antibody fragment affinity on nanoparticle targeting of epidermal growth factor receptor-expressing tumor cells. J Mol Biol. 2007; 371(4):934–947. [PubMed: 17602702]
8. Gu F, Zhang L, Teply BA, Mann N, Wang A, Radovic-Moreno AF, Langer R, Farokhzad OC. Precise engineering of targeted nanoparticles by using self-assembled biointegrated block copolymers. Proc. Natl. Acad. Sci. U. S. A. 2008; 105(7):2586–2591. [PubMed: 18272481]
9. Peer D, Karp JM, Hong S, Farokhzad OC, Margalit R, Langer R. Nanocarriers as an emerging platform for cancer therapy. Nat. Nanotechnol. 2007; 2(12):751–760. [PubMed: 18654426]
10. Fink-Retter A, Gschwantler-Kaulich D, Hudelist G, Mueller R, Kubista E, Czerwenka K, Singer CF. Differential spatial expression and activation pattern of egfr and her2 in human breast cancer. Oncol. Rep. 2007; 18(2):299–304. [PubMed: 17611648]
11. Taniguchi K, Okami J, Kodama K, Higashiyama M, Kato K. Intratumor heterogeneity of epidermal growth factor receptor mutations in lung cancer and its correlation to the response to gefitinib. Cancer Sci. 2008; 99(5):929–935. [PubMed: 18325048]
12. Dexter DL, Leith JT. Tumor heterogeneity and drug resistance. J. Clin. Oncol. 1986; 4(2):244–257. [PubMed: 3944607]
13. Muss HB, Thor AD, Berry DA, Kute T, Liu ET, Koerner F, Cirrincione CT, Budman DR, Wood WC, Barcos M, et al. C-erbb-2 expression and response to adjuvant therapy in women with node-positive early breast cancer. N. Engl. J. Med. 1994; 330(18):1260–1266. [PubMed: 7908410]
14. Parker N, Turk MJ, Westrick E, Lewis JD, Low PS, Leamon CP. Folate receptor expression in carcinomas and normal tissues determined by a quantitative radioligand binding assay. Anal. Biochem. 2005; 338(2):284–293. [PubMed: 15745749]
15. Dreher MR, Liu WG, Michelich CR, Dewhirst MW, Chilkoti A. Thermal cycling enhances the accumulation of a temperature-sensitive biopolymer in solid tumors. Cancer Res. 2007; 67(9): 4418–4424. [PubMed: 17483356]
16. Meyer DE, Kong GA, Dewhirst MW, Zalutsky MR, Chilkoti A. Targeting a genetically engineered elastin-like polypeptide to solid tumors by local hyperthermia. Cancer Res. 2001; 61(4):1548–1554. [PubMed: 11245464]
17. Meyer DE, Shin BC, Kong GA, Dewhirst MW, Chilkoti A. Drug targeting using thermally responsive polymers and local hyperthermia. J. Controlled Release. 2001; 74(1–3):213–224.
18. McDaniel JR, MacKay JA, Quiroz FG, Chilkoti A. Recursive directional ligation by plasmid reconstruction allows rapid and seamless cloning of oligomeric genes. Biomacromolecules. 2010; 11(4):944–952. [PubMed: 20184309]
19. Guda C, Zhang X, Mcpherson DT, Xu J, Cherry JH, Urry DW, Daniell H. Hyper expression of an environmentally friendly synthetic-polymer gene. Biotechnol. Lett. 1995; 17(7):745–750.

20. Liu WG, MacKay JA, Dreher MR, Chen MN, McDaniel JR, Simnick AJ, Callahan DJ, Zalutsky MR, Chilkoti A. Injectable intratumoral depot of thermally responsive polypeptide-radionuclide conjugates delays tumor progression in a mouse model. J. Controlled Release. 2010; 144(1):2–9.
21. MacKay JA, Callahan DJ, FitzGerald KN, Chilkoti A. Quantitative model of the phase behavior of recombinant pH-responsive elastin-like polypeptides. Biomacromolecules. 2010; 11(11):2873–2879.
22. Meyer DE, Chilkoti A. Quantification of the effects of chain length and concentration on the thermal behavior of elastin-like polypeptides. Biomacromolecules. 2004; 5(3):846–851. [PubMed: 15132671]
23. Mellman I, Fuchs R, Helenius A. Acidification of the endocytic and exocytic pathways. Annu Rev Biochem. 1986; 55:663–700. [PubMed: 2874766]
24. Roberts WG, Palade GE. Neovasculature induced by vascular endothelial growth factor is fenestrated. Cancer Res. 1997; 57(4):765–772. [PubMed: 9044858]
25. Yuan F, Dellian M, Fukumura D, Leunig M, Berk DA, Torchilin VP, Jain RK. Vascular-permeability in a human tumor xenograft - molecular-size dependence and cutoff size. Cancer Res. 1995; 55(17):3752–3756. [PubMed: 7641188]
26. Kong G, Braun RD, Dewhirst MW. Hyperthermia enables tumor-specific nanoparticle delivery: Effect of particle size. Cancer Res. 2000; 60(16):4440–4445. [PubMed: 10969790]
27. Liu WE, Dreher MR, Furgeson DY, Peixoto KV, Yuan H, Zalutsky MR, Chilkoti A. Tumor accumulation, degradation and pharmacokinetics of elastin-like polypeptides in nude mice. J. Controlled Release. 2006; 116(2):170–178.
28. Hatefi A, Amsden B. Biodegradable injectable in situ forming drug delivery systems. J. Controlled Release. 2002; 80(1–3):9–28.
29. Jeong B, Bae YH, Lee DS, Kim SW. Biodegradable block copolymers as injectable drug-delivery systems. Nature. 1997; 388(6645):860–862. [PubMed: 9278046]
30. Bidwell GL, Davis AN, Fokt I, Priebe W, Raucher D. A thermally targeted elastin-like polypeptide-doxorubicin conjugate overcomes drug resistance. Invest. New Drugs. 2007; 25(4): 313–326. [PubMed: 17483874]
31. Bidwell GL, Fokt I, Priebe W, Raucher D. Development of elastin-like polypeptide for thermally targeted delivery of doxorubicin. Biochem. Pharmacol. 2007; 73(5):620–631. [PubMed: 17161827]
32. Raucher D, Chilkoti A. Enhanced uptake of a thermally responsive polypeptide by tumor cells in response to its hyperthermia-mediated phase transition. Cancer Res. 2001; 61(19):7163–7170. [PubMed: 11585750]
33. Vagberg LJM, Cogan KA, Gast AP. Light-scattering study of starlike polymeric micelles. Macromolecules. 1991; 24(7):1670–1677.
34. Dewhirst MW, Vujaskovic Z, Jones E, Thrall D. Re-setting the biologic rationale for thermal therapy. Int. J. Hyperthermia. 2005; 21(8):779–790. [PubMed: 16338861]

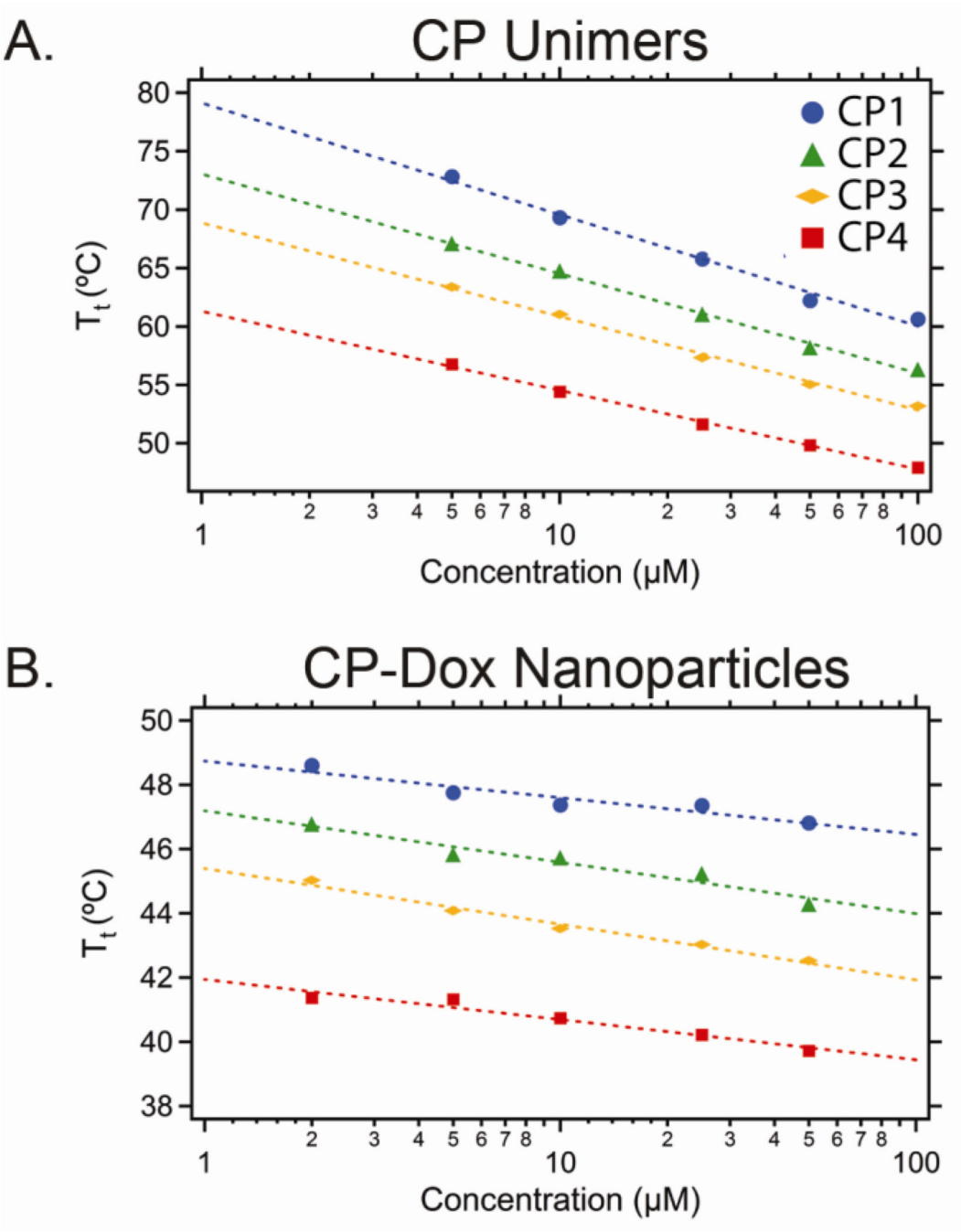

Figure 1.
Inverse transition temperature (T_t) of a series of: **(A)** CPs and **(B)** CP-Dox nanoparticles as a function of CP concentration in PBS. The dashed line represents the best fit.

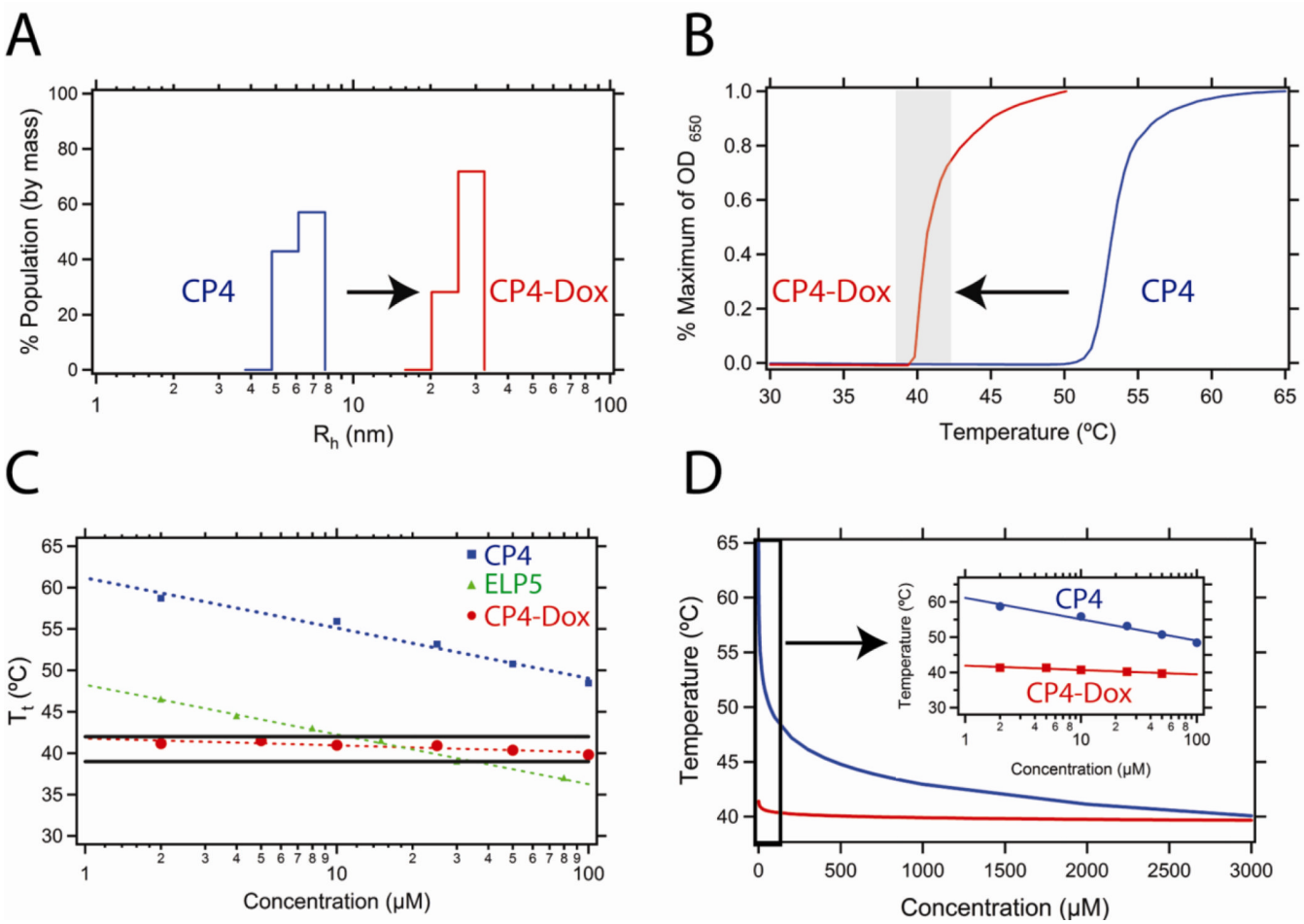

Figure 2.

(A) Dynamic light scattering results for the CP4 unimer without Dox conjugation (blue) and the CP-Dox nanoparticle (red) at 25 μM CP concentration in PBS at 25 °C. **(B)** Turbidity profiles of CP4 unimer without Dox conjugation (blue) and the CP-Dox nanoparticle (red) at 25 μM CP concentration in PBS. The shaded region indicates the hyperthermia window (39 – 42 °C) of interest for *in vivo* thermal targeting. **(C)** The CP4-Dox nanoparticle (red) shows virtually no dependence of its T_t on concentration and hence remains within the hyperthermia window (black lines) over a wide concentration range whereas the CP4 unimer (blue) and a CP unimer commonly used in previous hyperthermia studies (ELP5: green; $X=A_2G_3V_5$; data from [17]) show a strong concentration dependence and hence are thermally responsive over a narrow range of concentration. **(D)** Representative relationship between the T_t and the concentration for CP4 unimer (blue line) and the CP-Dox nanoparticle (red line). The inset displays a magnified view of the low concentration regime for the CP4 unimer and CP4-Dox nanoparticle.

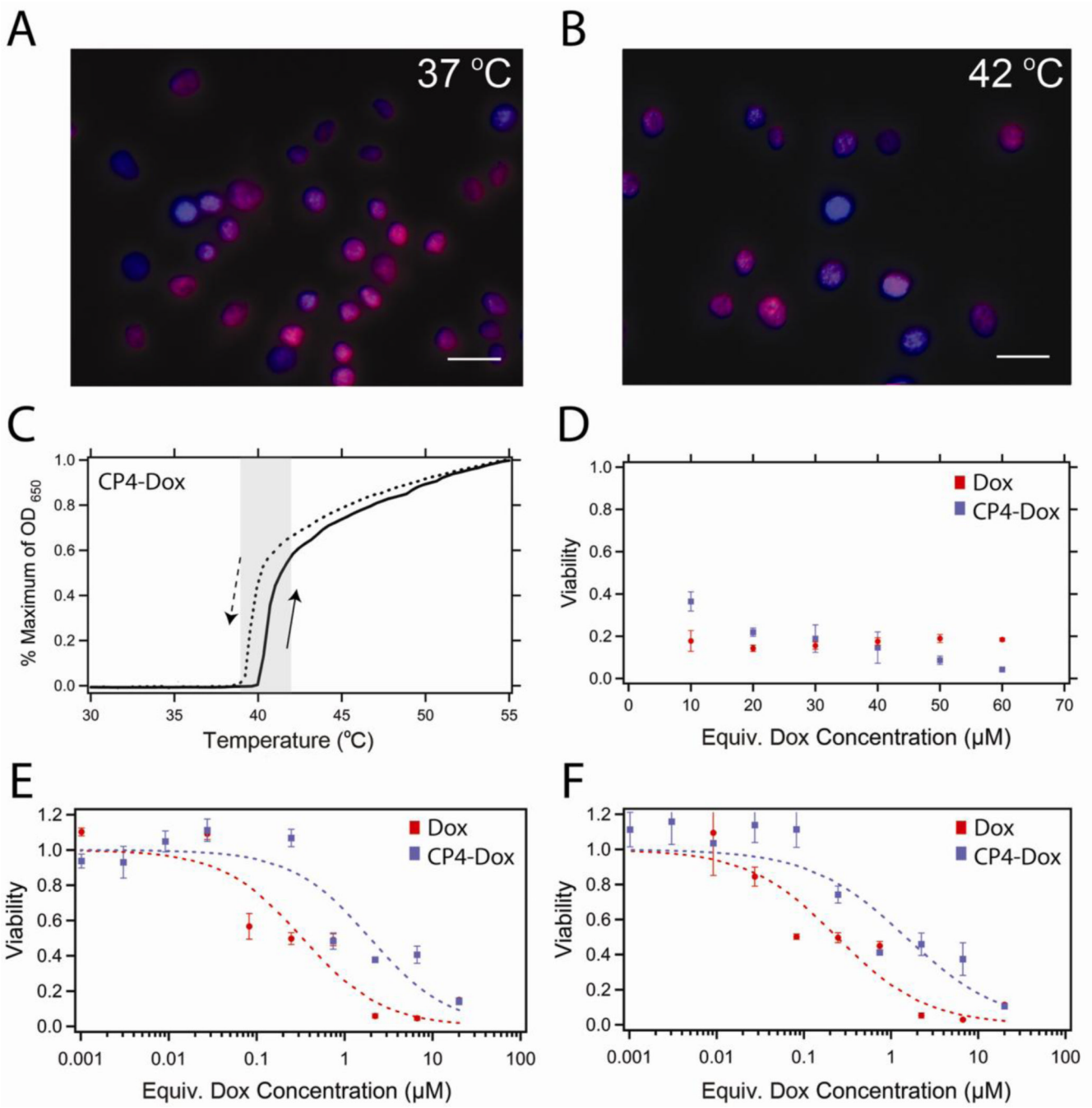

Figure 3.

In vitro cytotoxicity of CP-Dox nanoparticles. **(A)** Fluorescence microscopy of C26 cells following 1 h incubation at 37 °C or **(B)** 42 °C with CP-Dox nanoparticles at 5.6 μM (30 μM Dox equivalents). Colocalization of Dox (red) with Hoechst stain (blue) suggests that the Dox localizes to the nucleus with and without the application of heat. Scale bars indicate 25 μm. **(C)** The phase transition of CP4-Dox is fully reversible in complete cell media. CP4-Dox transitions within the hyperthermia window (shaded) at 40.2 °C at 25 μM CP. **(D)** Viability of C26 cells after mild hyperthermia (1 h at 42 °C) and 24 h incubation with Dox at 37 °C (red) or CP-Dox nanoparticles (blue). **(E)** Viability of C26 cells following a 1 h

exposure at 37 °C or **(F)** 42 °C and a 72 h incubation in Dox (red) or CP-Dox nanoparticles (blue). Concentrations below 0.1 μM likely result in the disassembly of the nanoparticle system.

Table I

CP libraries. CP libraries are described by their guest residue composition, number of pentapeptide repeats and the theoretical molecular weight of the CP incorporating both the leader (Ser-Lys-Gly-Pro-Gly) and the trailer [Cys(Gly-Gly-Cys)$_7$] sequences. CPs 1–4 are listed in order of increasing hydrophobicity.

	Xaa (A:V)	Pentamers	MW (Da)	Expressed
CP1	1:0	5	4315.8	
		10	6223	
		20	10037.3	
		40	17665.9	*
		80	32923.2	*
		160	63437.8	*
CP2	14:1	15	8158.2	
		30	13907.7	
		60	25406.8	*
		120	48404.9	
		150	59904	*
CP3	9:1	10	6251	
		20	10093.4	
		40	17778.2	*
		80	33147.6	*
		160	63886.6	*
CP4	4:1	5	4343.9	
		10	6279.1	
		20	10149.5	
		40	17890.4	*
		80	33372.1	*
		160	64335.5	*

The * indicates CPs that were expressed in *E. coli* from their plasmid-borne synthetic gene.

Table II

Hydrodynamic radius (R_h; 25 μM at 25 °C), conjugation efficiency and T_t (50 μM) in PBS and FBS for four CP-Dox conjugates.

	Pentamers	Rh (nm)	Dox/ELP	T_t (°C, PBS)	T_t (°C, FBS)
CP1-Dox	160	21.2	5.4	46.8	42.1
CP2-Dox	150	19.6	6.3	44.3	40.9
CP3-Dox	160	24.8	5.7	42.5	39.4
CP4-Dox	160	23.6	5.6	39.7	36.5